Swollen cubic phases with reduced hardness solubilizing a model fragrance oil as a co-surfactant

Vera Tchakalova, Thomas Zemb, Fabienne Testard

Swollen cubic phases with reduced hardness solubilizing a model fragrance oil as a co-surfactant

ⓘ Vera Tchakalova, ⓘ Thomas Zemb and Fabienne Testard

Swollen cubic phases with reduced hardness solubilizing a model fragrance oil as a co-surfactant

Vera Tchakalova[1, *], Thomas Zemb[2] and Fabienne Testard[3]

[1,*] Firmenich SA, R&D Division, Rue de la Bergère 7, CH-1242 Satigny, Switzerland

[2] Institut de chimie séparative, UMR 5257 CEA/CNRS/UM , Centre de Marcoule, F30207 Bagnols sur Ceze, France

[3] Université Paris-Saclay, CEA, CNRS, NIMBE, 91191 Gif-sur-Yvette Cedex, France

*Corresponding author: vera.tchakalova@firmenich.com

Abstract

Swollen cubic lyotropic ternary phases with Pn3m symmetry and reduced hardness were obtained from a specific binary mixture of cubic phase-forming (phytantriol) and lamellar phase-forming (decaglycerol monooleate) compounds. The microstructures were determined by using a small-angle X-ray scattering technique. The softness and temperature-induced phase transitions were investigated by means of rheology. The incorporation of a surface-active fragrance compound (linalool) at concentrations up to 6%wt induced a structural transition toward a softer Im3m bulk cubic phase with longer water channels. Higher linalool concentrations allowed the spontaneous dispersion of the bulk cubic phase into microscopic particles with a cubic structure (cubosomes).

Introduction

Cubic phases are widely used in pharmaceutical, therapeutic, food, cosmetics, biotechnology, and other industries.[1] The biocompatibility and bio-adhesiveness of cubic phases make them attractive soft delivery systems. They are particularly interesting for the controlled release of actives due to their ability to solubilize both hydrophobic and hydrophilic compounds. Their complex topology is a limiting factor for the diffusion of the entrapped solutes.[2] The literature

1

covering the solubilization and controlled release of drugs and hydrophilic actives in cubic phases is huge. Outstanding reviews summarize studies in this area.[3–5]

The solubilization of volatile fragrance or flavor compounds in bicontinuous cubic phases for controlled release is a domain that is still not sufficiently explored. Cubic phases and their dispersions – in the form of cubosome particles that include large quantities of fragrance composed of base, middle, and top olfactive notes, and a low quantity of biobased surface-active building blocks – are of special interest for green formulations of creams that do not lose their softness and have a delayed fragrance release. The volatility and small size of the volatile compounds hinders their efficient entrapment in a "soft" delivery system such as lyotropic amphiphilic structures. The various chemical functionalities of fragrance ingredients bearing different polarities and surface activities[6–10] strongly influence spontaneous curvature, as well as polar/apolar specific area per unit volume. Therefore, their inclusion induces phase transitions and changes in the melting point of the structure. Examples of such transitions in cubic phases are reported in the studies of Kanei et al. and Uddin et al., who describe the solubilization of fragrance compounds in a discontinuous cubic phase of type I_1, composed of micelles arranged in a cubic lattice.[11,12] In these studies, it was established that surface-active volatile molecules such as linalool participate to the volume of the palisade layer[13] as well to the effective area per molecule, by increasing the area per surfactant, and change the internal structure of the phase, inducing both the transition from I_1 to H_1 to L_α and a strong change in the melting temperature, in contrast to the activity of the highly hydrophobic compound limonene. In another study,[14] it was demonstrated that two different types of γ-lactones, solubilized in bicontinuous cubic phases at high concentrations (15-20%wt), influenced the phases differently: one of the lactones preserved the cubic phase, whereas the other transformed it to an inverted hexagonal phase. Food volatile compounds, including linalool at concentrations of 10 to 12%wt, were solubilized in the bicontinuous cubic phase of monoolein/water binary systems in the work reported by Amar-Zrihen et al., and a facilitated transition to the reverse hexagonal phase was observed.[15] Such a transition, *i.e.* from cubic to hexagonal phases, was also obtained with non-volatile oils such as tetradecane,[16] diolein,[17] oleic acid, and sodium oleate.[18] However, the phase transition was observed mainly when the cubic phases were built of non-ionic surfactants. The cubic phases of charged surfactants such as DDAB were not perturbed by the addition of oils with different polarities, even at a very high oil concentration.[19] These studies, therefore, emphasize that the phase transitions depend on both the polarity of the oils and the type of surfactants. Maddaford and Toprakcioglu clearly

highlighted that the phases adopt the structure, which minimizes the difference between the actual and preferred curvatures.[19] This confirms that the geometry of the phase, its curvature, transition, and melting point could be successfully tuned by a combination of surfactants with an appropriate spontaneous curvature and oils with adapted polarity. Such combination have been successfully used to incorporate a third uncharged component in an ultra-swollen lipid mesophases made of an anionic phospholipid and monoacylglycerol monopalmitolein.[20]

In this study, we report the formation of a soft bicontinous cubic phase of type Pn3m, with reduced viscosity, achieved by combining cubic phase-forming (phytantriol) and lamellar phase-forming (decaglycerol monooleate) compounds, capable of resisting the solubilization of a fragrance surface active volatile oil such as linalool. Interestingly, it was established that some fragrance compounds could play a role as hydrotropes in a similar manner to ethanol and could disperse the bulk cubic phase in microscopic particles (cubosomes) by spontaneous emulsification obtained upon dilution.

The studies on the cubic phases that solubilize fragrance and flavor compounds, discussed earlier, were performed mainly with monoolein as a cubic phase-forming surfactant.[21] The explanation for this choice is the low price and biocompatibility of the monoglycerol. In our study, we chose to explore the potential of phytantriol-water cubic phases due to the attractive advantage of phytantriol as a skin hydrating agent.[22]

Experimental

1. Materials

Phytantriol (3,7,11,15-tetramethylhexadecane-1,2,3-triol) was provided by DSM. Decaglycerol monooleate (10-GMO) (Polyaldo 10-1-0 K FG) is a product of Lonza Inc. (Allendale, NJ, USA). The fragrance ingredient linalool was provided by Firmenich SA, Switzerland. Table 1 summarizes the molar mass, density, and log P values of the different compounds.

Table 1: Characteristics of compounds of interest

	Molar mass (g/mol)	Density (g/cm^3)	Log P
Phytantriol	330.5	0.91	
10-GMO	1023.2	1.08	
Linalool	1542.2	0.87	2.97

3

2. Preparation of solutions

In a first series of experiments, mixtures of phytantriol and 10-GMO in water were prepared by the following method: 1) phytantriol and 10-GMO were mixed in the desired molar ratio by gentle agitation with a magnetic stirrer at 75°C; 2) preheated water was added, keeping the mixture at 75°C; and 3) the obtained mixtures were cooled to room temperature under agitation with an electromagnetic stirrer at 100 rpm. Solid, transparent gels were obtained below 40°C and were stable at room temperature for several months.

In a second series of experiments, a fragrance ingredient was added to the cubic phase prepared with the mixture of phytantriol, 10-GMO, and 30%wt water, as described above, and integrated by gentle agitation.

3. Small-angle X-ray scattering measurements

Small-angle X-ray scattering (SAXS) measurements were performed on a Huxley-Holmes high-flux camera equipped with a copper rotating anode operating at 15 kW and a Xenocs monochromator mirror (or collimation optics) to select the Kα_1 radiation (at $\lambda = 1.5418$Å).[23,24] Data were recorded on a two-dimensional MAR300 image plate detector positioned at 120 cm from the sample holder, ensuring a q-range of 0.015 to 0.6 Å^{-1}. Data correction, radial averaging, and absolute scaling were performed with routine procedures.[24] The measurements were performed in transmission geometry with 1.5 mm borosilicate capillaries for the solution and sticky Kapton cells for the gels with a typical acquisition time of 7200 s.

One pattern (Fig 1 A) has been obtained on a different set-up from SWAXS-Lab in Paris Saclay. A SAXS high brilliance apparatus (CEA design) equipped with a Xenocs Genix microsource ($\lambda = 1.54$ Å) coupled with a long distance focalization optics and a Dectris Pilatus 200K detector. The sample to detector distance of 114 cm gives a q-range of 0.01 to 0.35 Å^{-1}. Data treatment for image averaging and normalization were performed with PYSAXS, an open source python package (https://pypi.org/project/pySAXS/). The counting time for the cubic mesophase (30% water) presented in Fig 1 A is 1800s, although Bragg peaks appear after 30s.

4. Rheology

Flow and oscillatory rheology were used to study the viscoelastic behavior of the samples. Rheological experiments were performed at 25 °C with a TA Instruments AR 1500. The experimental parameters were fixed with the software AR Instrument Control. The flow experiments were performed with an aluminum cone device with a diameter of 40 mm and an angle of 4°. This geometry was chosen to assure uniform stress all along the sheared surface independently of the diametric position. The gap between the cone geometry and the deposition plate was fixed instrumentally at a value of 100 µm. The flow experiment was a shear ramp test with a controlled rate. The shear rate varied from 0.01 to 1000 s^{-1} in log scale with 10 points/decade. Shear stress as a function of shear rate revealed the flow behavior of the studied samples.

For the oscillatory rheology, steel plate geometry with a diameter of 40 mm was used with a gap of 500 µm. The first step was to perform a stress sweep in the range 10^{-4} to 10^5 Pa at different frequencies (ω = 1, 10, 100 rad/s) to find the linear part of each dependence of elastic modulus G` as a function of the applied stress. The second step was to perform a frequency sweep at a fixed stress (0.1 Pa) chosen from the linear part of the stress sweep, in the frequency range $\omega \in$ 0.1-500 rad/s with 10 points/decade in log scale.

The viscoelastic behavior of the samples was studied by applying sinusoidal deformations (strain) at different angular frequencies (ω). The shear stress developed by the system in response to the deformations was also sinusoidal, which is out of phase with the strain. The complex shear modulus was $G^*=G$`$+iG$``, where $G$` and $G$`` are defined as storage and loss moduli, respectively. The elasticity (G`) and the viscosity (G``) of the material are expressed by these two moduli. The oscillatory curves allowed us to determine different structural parameters, such as the relaxation time and mesh size of the network.

Results

1. Cubic gel formed by a mixture of phytantriol and decaglycerol monooleate
    1.1 SAXS studies

1.1.1 Binary phytantriol in water system

Phytantriol is an amphiphilic branched triol, which is known to predominantly form cubic phases in binary solution with water; the binary phase diagram was determined by Barauskas and Landh.[25] At room temperature, lamellar phase L$_\alpha$ exists at water concentrations between 6 and 13%wt, followed by the body-centered cubic phase of space group Ia3d (Q230) in the water

concentration range between 14 and 23%wt, and then followed by the bicontinuous cubic phase with a space group Pn3m (Q224) in the very narrow water concentration range between 26 and 28%wt. The presence of higher water content leads to the expulsion of water as an excess phase due to an emulsification failure, indicating, on one hand, reversed phase and, on the other, saturation of the water channels. The scattering studies of these cubic phases revealed lattice parameters varying from 86 to 100 Å for the Ia3d phase in the corresponding water concentration range and from 64 to 66 Å for the Pn3m phase in the water range between 26 and 28%wt.[25] A narrow range of phase existence is linked to high rigidity of the molecular thick layer.[26]

For our studies, we started with SAXS analysis of the binary phytantriol-water mixtures at three water concentrations (22%wt, 27%wt, and 30%wt) and at room temperature (25°C) in order to confirm the structure of our reference system before the incorporation of additional molecules (10-GMO and fragrance oil). The scattering profiles approved the sequence of cubic phases – Ia3d (Q230, gyroid), Pn3m (Q224, diamond), and Pn3m + excess water – as reported by Barauskas and Landh.[25]

The lattice parameter of the cubic phases could be calculated from the Bragg peaks (q_{hkl}) or the repeat distance d^* (see Figure SI.1.1 in the supplementary Information section (SI)). The indexation for all cubic phases could be found in the *Handbook of Applied Surface and Colloidal Chemistry*.[27]

The lattice parameter of the Ia3d cubic phase of the binary phytantriol-water system at 22% water content was 96.2 Å, whereas the lattice parameter of the Pn3m phase at 27%wt water was 64.4 Å, in good accordance with the previously calculated lattice parameters and confirming the correct structure of our reference phase. At 30%wt water, the Pn3m phase was obtained in equilibrium with excess water, and it is at maximum swelling. Since the cubic phase is in equilibrium with excess water, the osmotic pressure is zero: a situation described as "fully hydrated". Note that at this point the number of molecules in the palisade layer is the same as in non-fully hydrated situation: the amount of water is determined by the hydration forces.[28] The cubic phase was analyzed after removing the excess water by centrifugation. The lattice parameter was calculated to be 65.8 Å.

The swelling law for the cubic phases follows the equation (1):

$$\log\left(\frac{d*}{l} - 1\right) \propto -s' \log(\emptyset_{polar}), \qquad (1)$$

6

where s' is the molecular shape parameter of the polar phase, d* is the repeat spacing, l is the molten chain length of the amphiphile and Φ_{polar} is the volume fraction of the polar phase.

1.1.2 Binary 10-GMO in water system

10-GMO is an amphiphilic molecule, forming essentially lamellar phases.[29] The SAXS profiles of the binary system 10-GMO-water at different water concentrations (see Figure SI1.1 in SI) confirmed the lamellar structure. Increasing the water content led to better organization of the lamellar phase with an increasing repeat distance (d*) from 61 (at 5% water) to 157 Å (at 66% water).

For the lamellar phase, the dilution law $d^* = \frac{2l}{\emptyset_l}$ allowed us to directly determine the bilayer thickness (d$_l$ = 2l) and surfactant length (l) by knowing the volume fraction Φ_l of 10-GMO. Thus, the bilayer thickness, including the polar heads of the surfactant, was deduced from the slope of the linear fit of the dependence (d^*=f(Φ_l)) and was 54 Å (Figure SI.1.2 in SI). Therefore, l had a value of 27 Å corresponding to the molecular length of the whole 10-GMO in the current arrangement. The hydrophobic chain length of monoolein[30] was reported to be 17 Å at 20°C. Therefore, the length of the polar part of 10-GMO should be 10 Å, which indicates that the long glycerol chain is not extended, confirming what was already supposed by Guo et al.[29] Since the molecular volume is known from the density and molar mass to be 1573 Å^3/molecule, we determined the area per 10-GMO to be 58 Å^2.

1.1.3 Ternary mixtures of phytantriol and 10-GMO in water

Mixtures of phytantriol and 10-GMO in water at two different molar ratios (9:1) and (3:1) were studied to understand the influence of the lamellar phase-forming surfactant on the cubic phase of phytantriol. g

The scattering intensity profiles of the binary mixtures phytantriol-water and 10-GMO-water and the ternary mixture phytantriol-10-GMO-water at a fixed water concentration (30%wt) and surfactant molar ratio (3:1) are presented in Figure 1. The scattering intensity profile of the ternary mixture phytantriol-10-GMO-water at a fixed water concentration (30%wt) and the surfactant molar ratio (9:1) is included in the SI (Figure SI.1.3)

7

The mixture of phytantriol and 10-GMO at molar ratios 9:1 and 3:1 led to the formation of a reversed bicontinuous cubic phase of type Pn3m (D-surface) (Q224), identified by the six
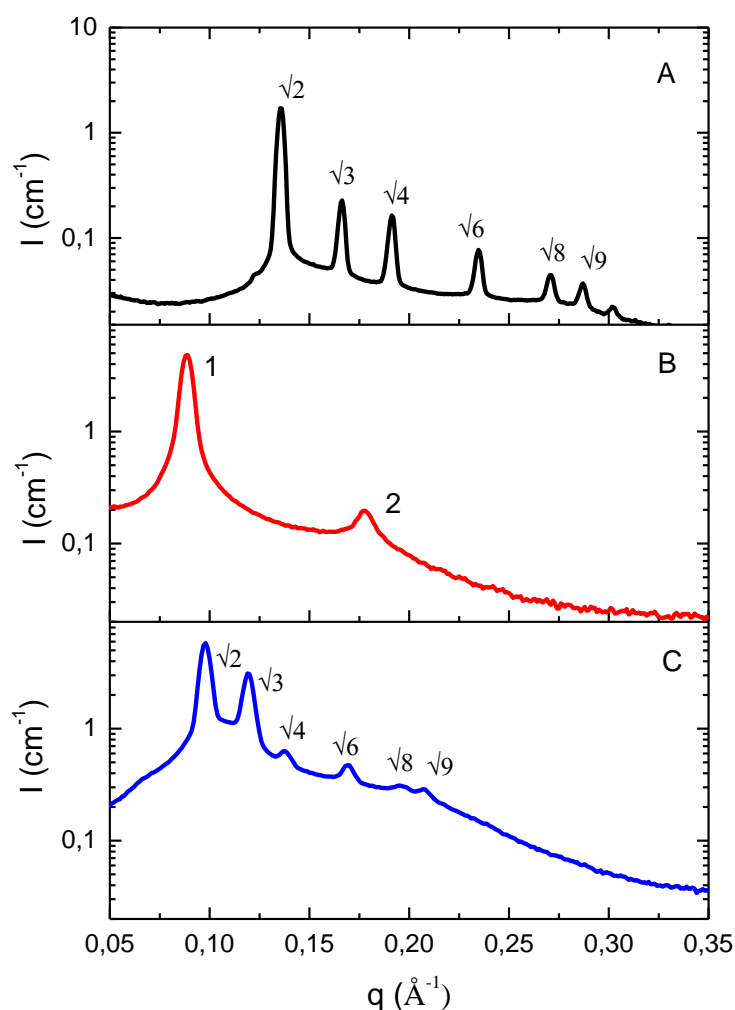

Figure 1 SAXS profiles of the binary mixtures of (A) phytantriol in 30%wt water and (B) 10-GMO in 30%wt water and the ternary mixture of (C) phytantriol-10-GMO at a 3:1 molar ratio in 30%wt water. Phytantriol is organized in a cubic phase, Pn3m (Q224), whereas 10-GMO is organized in a lamellar phase. The pattern in (A) corresponding to the sample phytantriol+30%wt water was obtained with different set-up (see Experimental section 3.)

Bragg peaks, following the relationships $\sqrt{2}:\sqrt{3}:\sqrt{4}:\sqrt{6}:\sqrt{8}:\sqrt{9}$. The incorporation of 10-GMO into the phytantriol bilayers increased the unit cell lattice parameter (Figure 2) from 65.8 Å for the binary (phytantriol-water) cubic phase to 73 Å and 91 Å for the mixed cubic phases at surfactant molar ratios of 9:1 and 3:1, respectively.

Therefore, when part of the phytantriol is replaced by 10-GMO, the Pn3m structure is preserved with consequently extended water channels.

8

The scattering curves, corresponding to the mixture of phytantriol and 10-GMO at a molar ratio of 3:1 at different water concentrations, are presented in Figure 3. At 10%wt water (Figure 3A), the phase is a microemulsion, which can be considered a molten cubic phase characterized by a single large peak on the scattering curve located at $d^*=2\pi/q_{max}=45.9$ Å. This microemulsion
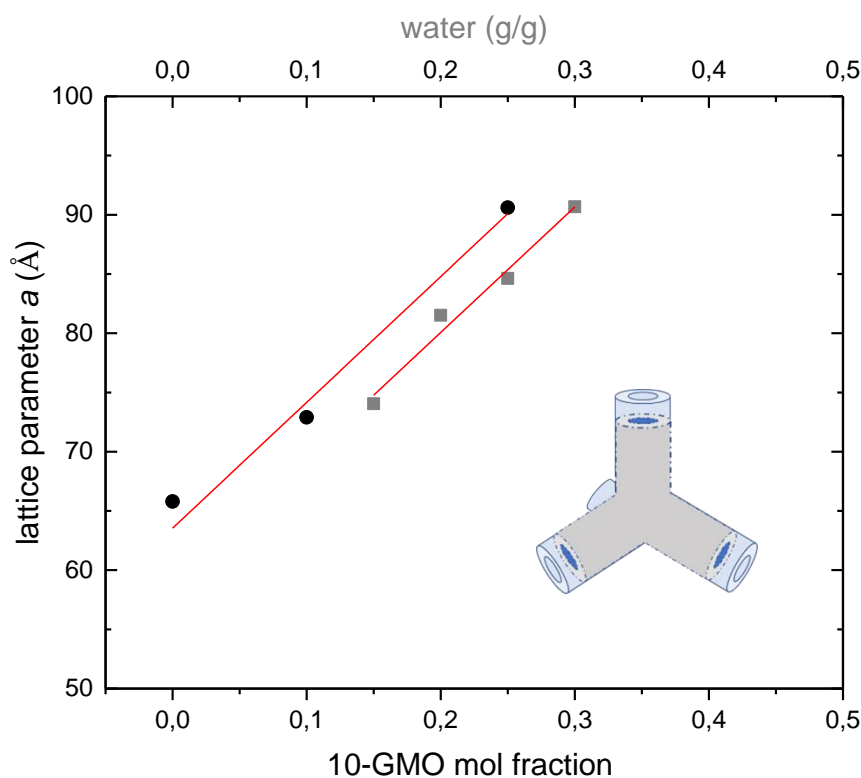

Figure 2 Lattice parameter of the Pn3m cubic phase of ternary phytantriol-10-GMO-water mixtures as function of 10-GMO molar fraction in the mixture phytantriol-10-GMO (black circles) at 30%wt water and of the water concentration (gray squares) for 3:1 phytantriol-10-GMO molar ratio.

is of a type disordered open connected (DOC) cylinders with Z3 or Z4.[31] From 15%wt (Figure 3B) up to 30%wt water (Figure 3E), the scattering profiles revealed a cubic Pn3m, D, Q224 structure. At water concentrations higher than 30%wt, a second excess water phase co-exists in equilibrium with the Pn3m phase. The analysis of the cubic phase at 50%wt water (after the removal of the water excess phase by centrifugation) (Figure 3F) revealed the appearance of an additional peak at very low q-values (q = 0.07 Å^{-1}).

The first advantage of the formation of mixed (phytantriol-10-GMO) bilayers is the extension of the Pn3m phase domain from 15 to 30%wt water compared with the single-component phytantriol bilayers, the latter forming this phase in a very narrow region (26%-28% water; see the binary phase diagram in Reference[25]) before saturation of the water channels. The Ia3d cubic phase, which is presented on the binary phase diagram (phytantriol-water) in the water concentration range 14 to 23%wt, disappeared and was replaced by the Pn3m cubic phase for the ternary mixture.
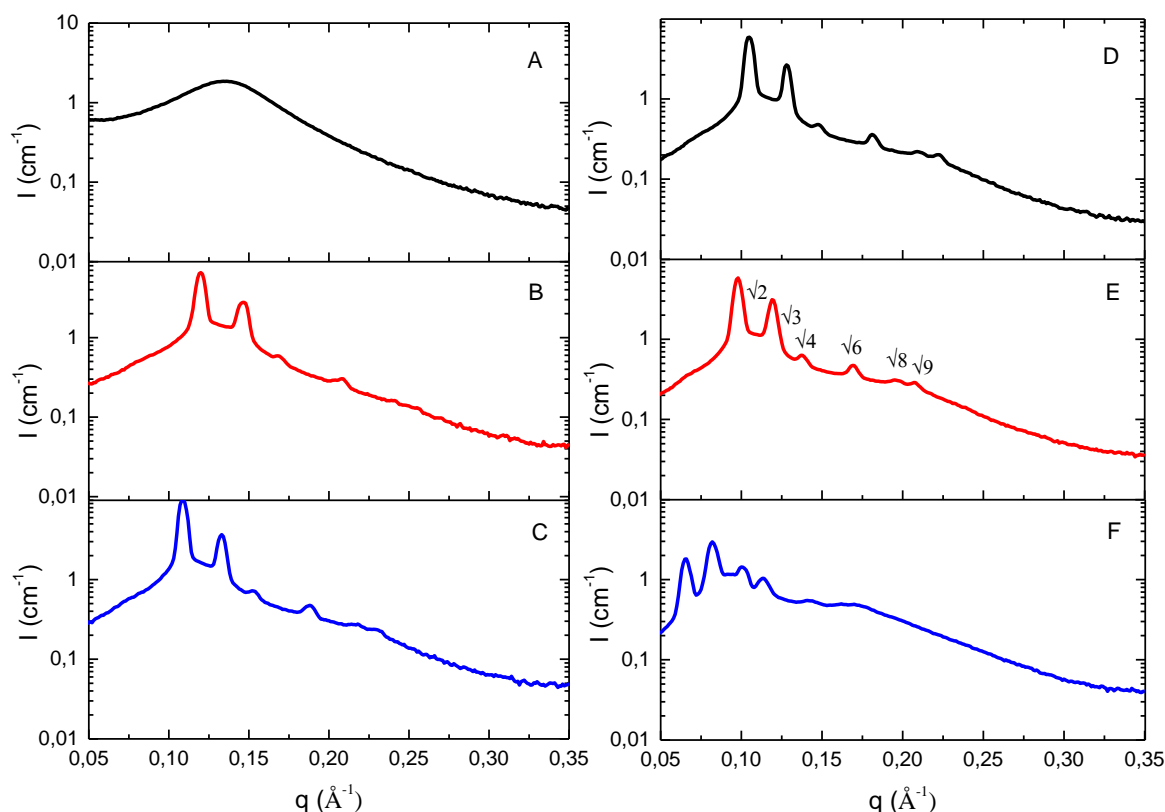

Figure 3 Scattering profiles of ternary phytantriol-10-GMO mixtures (3:1) as a function of (A) 10%wt, (B) 15%wt, (C) 20%wt, (D) 25%wt, (E) 30%wt, and (F) 50%wt water content.

The structural parameters, such as monolayer length, length of the rods forming the structure, radius of water channels, surface area of the minimal surface, and mean Gaussian curvature, were calculated and are reported in Table 2 for the binary phytantriol water system and in Table 3 for the mixtures.

The length of the lipid monolayer (including the whole surfactant molecule) was calculated from the surfactant composition (Φ_l) and the lattice parameter a by using the following equation:[30,32]

$$\emptyset_l = 2A_0 \left(\frac{l}{a}\right) + \frac{4\pi\chi}{3}\left(\frac{l}{a}\right)^3 \quad (2)$$

10

where Φ_l is the surfactant volume fraction, and A_0 and χ are the ratio of the minimal surface in a unit cell to the quantity (unit cell volume)$^{2/3}$ and the Euler-Poincaré characteristic, respectively, and have values specific for the different cubic phases (Pn3m: A_0=1,919 and χ=-2, Ia3d: A_0=3,091 and χ=-8, and Im3m: A_0=2,345 and χ=-4). The effective length of the lipid monolayer was calculated for each composition and the average length, which is 18.9±0.5 Å, can be assumed as independent of the composition. The mixed monolayer was thicker than that of the single phytantriol monolayer, for which l was calculated as 13.9 Å (using the data of Barauskas et al.[25]). For the mixture of phytantriol:10-GMO in the molar ratio 3:1, the volume of the lipid chain represent 59% of the volume of the lipids. From the volume fraction of lipid chains, the length of the lipid chain monolayer can be calculated for each composition. The average value equal to 10±0.25 Å can be assumed as constant in the water concentration range of Pn3m.

For the determination of the radius of the water channels, two approaches exist: IPMS (Infinite Periodic Minimal Surface) and geometrical, but it was demonstrated that both evaluation methods result in a similar water channel radius (±1 Å). Here, we used the second approach, and the radius of the water channels was calculated from geometrical considerations, describing the phase Pn3m as a network of water-filled rod-like channels of finite length. The number of water channels meeting each other in a unit cell for Pn3m phase is 4 (tetrahedral connection).[33] Thus, the radius of the water channels (r_w) is presented by the following equation:[30]

$$\emptyset_w a^3 = 4\pi r_w^2 l_r (1 - 0.78 \frac{r_w}{l_r}) \qquad (3)$$

where $\emptyset_w$ is the volume fraction of water, a is the lattice parameter, and l_r is the length of the rods, which could be calculated from the lattice parameter as $\frac{\sqrt{3}}{2} a$ for the Pn3m structure ($1/\sqrt{8}$ for Ia3d and 1 for Im3m structures). When the volume fraction of water is used, the radius of the water channel does not include the surfactant polar heads.

For the ternary Pn3m phase at surfactant molar ratio (phytantriol:10-GMO = 3:1), the radius of the water channels increased from 7.0 Å to 17.2 Å when the lattice parameter of the phase was increased from 66.8 Å (at 15% water) to 90.7 Å (at 30% water) (Figure 4). For comparison, in the single phytantriol cubic phase, the water channel radius was calculated as 11,9 Å at water content 30%wt (fully hydrated phase). Therefore, the mixed phytantriol-10-GMO system allowed us to considerably increase the water channel radius and to incorporate a higher

quantity of water inside. This could be useful for solubilization of water-soluble cosmetic actives, for example.
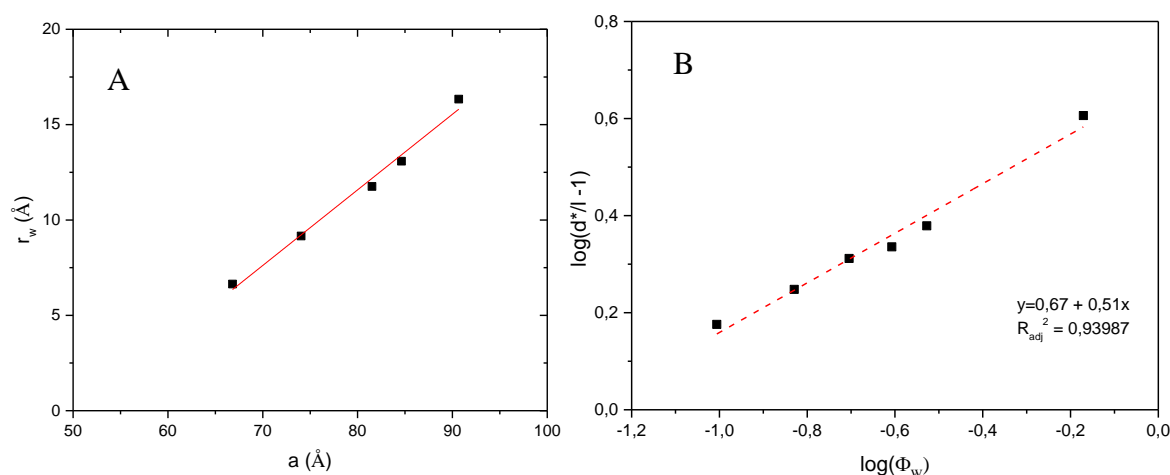

Figure 4 (A) Water channel radius r_w *as a function of lattice parameter* a. *(B) Swelling of the cubic phase as a function of water content according to equation (1).*

The mean Gaussian curvature can be calculated by knowing the lattice parameter *a* and using the following equation[30]:

$$\langle K \rangle_0 = \frac{2\pi\chi}{A_0 a^2} \qquad (4)$$

The mean Gaussian curvature is the curvature averaged on the unit cell and over the minimal surface. The mean curvature $\langle H \rangle_0$ over the minimal surface is zero.

The Gaussian curvature decreases, *i.e.* becomes less negative, increasing the water quantity in the mixed cubic phase, which indicates that the Pn3m mixed phase swells with the water concentration. The comparison of the Gaussian curvature of the mixed cubic phase (phytantriol-10-GMO) ($\langle K \rangle_0 = -0.00080$) to that of the cubic phase of phytantriol ($\langle K \rangle_0 = -0.0015$) at a water concentration corresponding to the water channel saturation shows that the incorporation of the lamellar phase-forming surfactant in the bilayer of phytantriol decreased by twice the mean Gaussian curvature of the mixed cubic phase.

The surface area of the lipid-water interface per unit cell (A), could be calculated from the lattice parameter *a* and by using the following equation:

$$A(\varepsilon) = A_0 a^2 + 2\pi\chi\varepsilon^2 \qquad (5)$$

where ε is the distance from the pivotal surface to the chain termini and at the minimal surface, is considered[34] equal to *l,* is also extended twice by the presence of the lamellar-forming lipid at 30%wt water content.

12

The cross section area per lipid at the lipid/water interface can be extracted by dividing $A(\varepsilon)$ by the number of lipid per unit cell:[35]

$$A_{cs}(\varepsilon) = \frac{2\,A(\varepsilon)v_l}{\Phi_{lch}\,a^3} \qquad (6)$$

The cross section area per polar head of lipid at polar/apolar interface can be calculated by taking into account the volume fraction of the lipid chains ($v_{l\text{-}ch}$), the volume of lipid chains per lipid and the length of the apolar part of the monolayer (indicated by a subscript "ch" in Table 2 and 3). Using the deduced parameters, the effective packing parameter can be estimated as $P_{eff\text{-}lch} = \frac{v_{l-ch}}{A_{cs\_lch}l_{ch}}$.

The packing parameter was calculated by knowing the Gaussian curvature:[36]

$$\langle K \rangle_0 = \frac{3}{2l^2}\,(1 - P_{eff}) \qquad (7)$$

where the effective packing parameter is expressed as $(v/al)_{eff}$. The values for all studied samples are included in Tables 2 and 3.

Table 2. Structural parameters of the phytantriol-water cubic phases. The weight water fraction "water%", the lattice parameter "a", the repeat distance "d*, the lipid length "l", the lipid chain length 'l$_{ch}$",the radius of the water channels "rw", the cross-sectional area per lipid at two distances l and lch "Acs_l" and "Acs_lch" respectively, the Gaussian curvature "<K>$_0$, the effective packing parameter "Peff".

Phytantriol in water										
Phase	Water %	d* (Å)	a (Å)	l (Å)	lch* (Å)	rw (Å)	<K>$_0$	Peff-l	Acs_l (Å^2)	Peff-lch	Acs_lch (Å
Ia3d	22	39,3	96,2	14,1	11,5	29,1	-0,0018	1,23	35,0	1,15	38,8
Pn3m	27	45,5	64,4	13,9	11,6	10,6	-0,0016	1,20	35,6	1,15	39,0

With the Euler-Poincare characteristic (Ia3d: A$_0$=3.091 and χ=-8 and Pn3m: A$_0$=1.919 and χ=-2)

Table 3. Structural parameters of the mixed phytantriol-10-GMO Pn3m cubic phase. The weight water fraction "water%", the repeat distance "d*, the lattice parameter "a", the lipid length "l", the lipid chain length 'l$_{ch}$",the radius of the water channels "rw" taking into account only the water contribution and not the polar head of the lipids, the cross-sectional area per lipid "Acs" at two distances l and lch, the Gaussian curvature "<K>$_0$, the effective packing parameter "Peff" for the 2 distances l and lch.

Phytantriol+10-GMO in water										
Phase	Water %	d* (Å)	a (Å)	l (Å)	lch* (Å)	rw (Å)	<K>$_0$	Peff-l	Acs_l (Å^2)	Peff-lch	Acs_lch (Å2
Pn3m	10	47,2	66,8	19,1	15,2	7,0	-0,0015	1,35	43,5	1,23	35,6
Pn3m	15	52,4	74,0	19,3	15,6	9,6	-0,0012	1,30	45,1	1,19	35,5
Pn3m	20	57,6	81,5	19,5	16,0	12,4	-0,0010	1,25	46,4	1,17	35,5
Pn3m	25	59,8	84,6	18,5	15,4	14,5	-0,0009	1,21	50,3	1,14	37,7
Pn3m	30	64,1	90,7	18,2	15,2	17,2	-0,0008	1,17	52,6	1,12	38,8

(*) l$_{ch}$ chain is calculated from eq (2) with the volume fraction of the lipid chains. For the pseudo-component phytantriol:10-GMO (3:1 molar ratio) the density is 1 and the chain in the lipid represents 59%v/v of the lipid.

The compositional expansion coefficient β (ppm^{-1}) was calculated for the mixed Pn3m phase by using the dependence of the lattice parameter on water content and the following equation:[30]

$$\beta = \frac{1}{a} * \left(\frac{\Delta a}{\Delta W}\right) \qquad\qquad (8)$$

where a is the lattice parameter at the water concentration of interest (30%wt water here) and ($\Delta a/\Delta W$) is the slope of the linear dependence a = f(water content) (Figure 2) in the range of water concentrations corresponding to the Pn3m phase. The higher expansion coefficient found for the cubic phase with mixed bilayers (β = 11685 ppm^{-1}), compared with that for the cubic phase with phytantriol bilayers (β = 7575 ppm^{-1}, at 28%wt), suggests higher flexibility of the mixed bilayers.

1.2 Rheological studies

The viscoelastic behavior of the mixed cubic phase was studied by oscillatory rheology; the comparison to the phytantriol cubic gel is presented in Figure 5.

It can be easily observed that both cubic gels express the typical viscoelasticity of the structured fluids with a well-determined rubbery plateau characterized by G` > G`` in a large frequency region. The values of both moduli are very high and have the typical values for the cubic phases[37] of the order of magnitude of $10^5$ to $10^6$ Pa. In general, the dependence of both modulus G` and G`` of the frequency can be described analytically by the Maxwell model, which consists of presenting the system as a combination of the mechanical pair spring and dashpot. From this model, the longest relaxation time and the zero-shear viscosity could be determined. However, it was already established that the cubic phases are complex viscoelastic systems, and for them the multiple Maxwell model should be applied, allowing determination of a couple of relaxation times, corresponding to different relaxation mechanisms. The interpretation of these relaxation mechanisms is still under debate. For this reason, we decided to limit our interpretation to a single relaxation time, which can be easily calculated from the frequency value "ω_{cr}" of the crossing point of G` and G``: $\tau_{max} = 1/\omega_{cr}$. This parameter represents the time needed for the relaxation of the water-bilayer interfaces to their initial configuration before the perturbation by the applied shear.

The longest relaxation time reflects the diffusion rate of the lipid molecules on the water-lipid interface.[34] Comparing the data for both cubic gels, one can see that the relaxation time of the
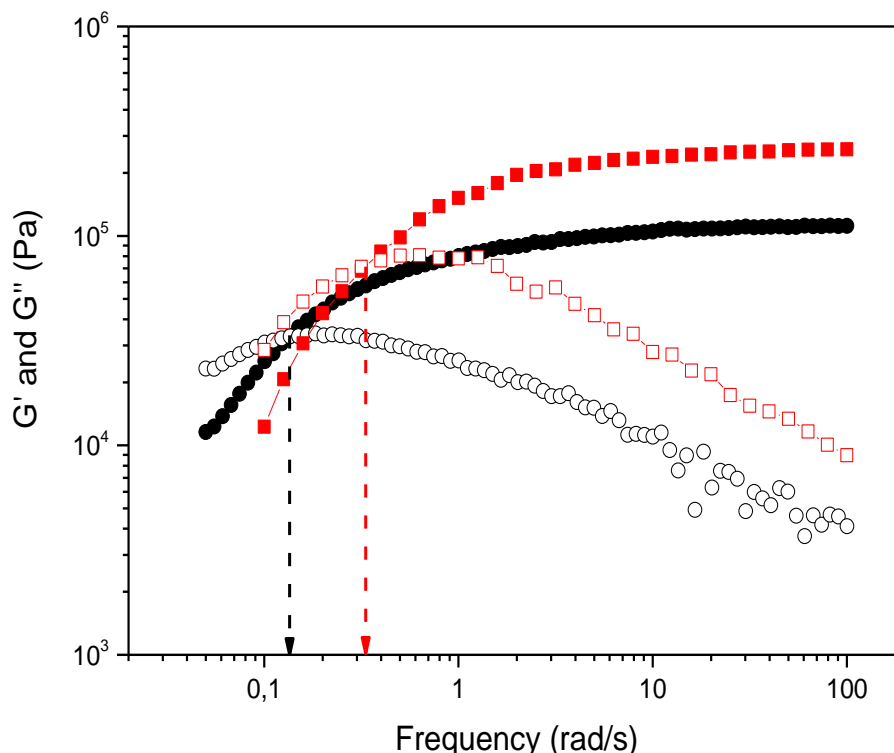

Figure 5 Viscoelasticity of a) mixed phytantriol-10-GMO (3:1 molar ratio) -water cubic gel (black) and b) phytantriol cubic gel (red) at 30% water. Full symbol for G` and empty symbol for G``.

mixed cubic gel (6.7 s) is 2 times longer than that of the cubic phytantriol gel (3.1 s) for similar water content (30%wt) and saturated water channels. Therefore, on the one hand, this result indicates slower surface diffusion of the surfactant molecules integrated into the mixed bilayers. On the other hand, the value of the plateau storage modulus G_0 of the mixed cubic phase (1.1×10^5 Pa) is more than 2 times lower than that of the phytantriol cubic phase (2.5×10^5 Pa), which is a sign of lower strength and mechanical rigidity of the mixed cubic gel. From these results, one can conclude that the mixed cubic gel is softer that the phytantriol cubic gel, but that the mixed bilayers need more time to relax to the initial configuration when the system is perturbated by an external deformation.

The temperature dependence of the viscoelasticity of the cubic gels is presented in Figure 6. Both G` and G`` followed the same behavior as a function of temperature for both gels. The
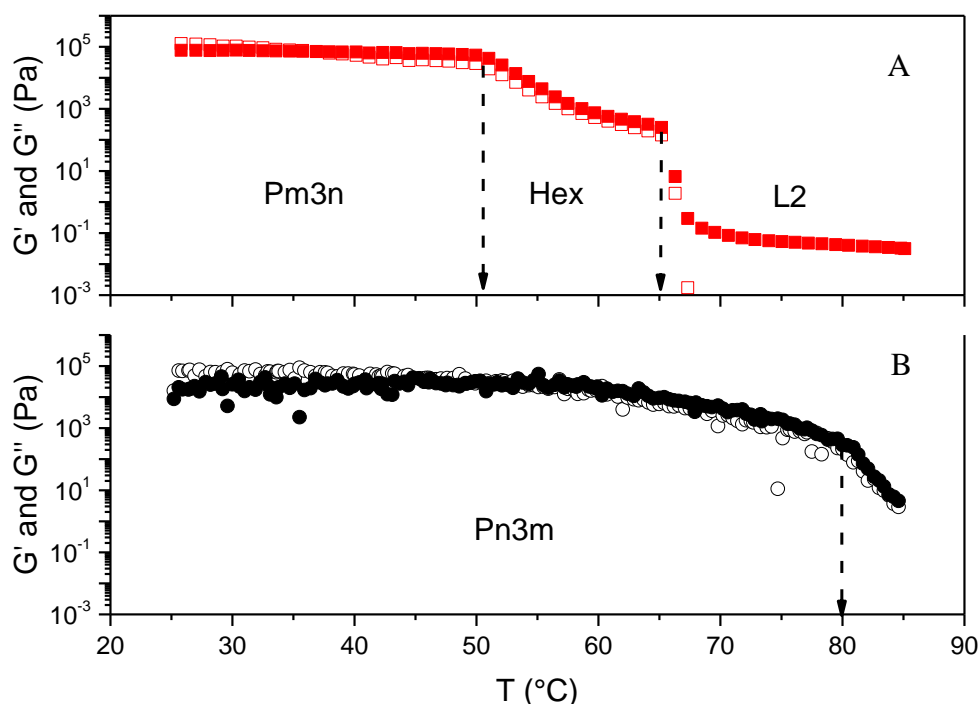

Figure 6 Influence of T on the viscoelasticity of the cubic phase: (A) phytantriol and (B) phytantriol-10-GMO (3:1 molar ratio).

phytantriol cubic Pn3m phase undergoes two phase transitions, at 50°C and at 65°C, which, according to the phase diagram included in the article by Barauskas et al.,[25] could be identified as Pn3m to H_{II} and H_{II} to L_2 phases. At a molecular level, these transitions in mesophases can be followed through molecular dynamics of lipid and water during the phase transitions as shown recently by Yao and Mezzenga et al in monolinolein-based lipidic mesophases.[38] The mixed Pn3m cubic gel showed remarkably stable viscoelastic behavior against temperature. No phase transitions were observed as a function of temperature for the mixed cubic gel up to 80°C. In other words, 10-GMO reinforces the phytantriol cubic phase against T changes. This result is important for the practical use of the present system.

In summary, in the first part of the study, the main advantages of the mixed 10-GMO-phytantriol-water system are as follows: a) conservation of the Pn3m structure, b) extension of the cubic phase domain in a larger water concentration range, c) increase in the water channel radius, d) formation of a softer Pn3m phase, and e) temperature stability of the mixed cubic Pn3m phase over a large temperature range (up to 80°C).

2. Incorporation of the fragranced alcohol (linalool) in the mixed cubic gel

2.1 SAXS studies

The peculiar property and main advantage in applications of the cubic phases for controlled release is their structural ability to "encapsulate" both polar and apolar actives. The polar molecules are solubilized in the water channels and their release depends on the topology of the phase and the interaction between the active and the water-lipid interface. The apolar molecules are placed mainly in the hydrophobic part of the bilayer. From previous studies concerning the solubilization of fragrance molecules in microemulsions,[6–8] we know that the partition of the fragrance oil between the different compartments – polar, apolar, or interface – depends on the fragrance ingredient functionality. The fragrance alcohols are strongly surface-active molecules, and they usually induce curvature changes and, consequently, phase transitions. In this way, they behave as co-surfactants. Therefore, it is interesting to investigate the role of such volatile surface-active molecules in the stability of the cubic phase.

Linalool is a fragrance alcohol with a specific surface activity. It was added to the already formed cubic phase, composed of the mixture of phytantriol-10-GMO in a 3:1 molar ratio and 30%wt water, as a "fourth" compound at different concentrations from 2 to 10%wt. The addition of the oil led to the formation of gels, the structure of which was analyzed by SAXS. The scattering profiles and 2D patterns are included in Figure 7. Samples with 2 and 4%wt linalool were presented in the form of bulk gels and the scattering studies performed directly. The samples at 6, 8, and 10%wt were presented in the form of a dispersion of gelified particles. For this reason, they were centrifuged, and the gel phase was extracted and analyzed by SAXS.

The scattering curves of the gels containing 4 and 6%wt of linalool contain Bragg peaks, the positions of which are in the ratios $\sqrt{2}:\sqrt{4}:\sqrt{6}:\sqrt{8}:\sqrt{10}$, corresponding to the 6-folded Im3m (primitive) cubic phase. Increasing the linalool concentration above 6%wt led to the disappearance of the Bragg peaks, which is a sign of local order softening, inducing the transformation of the mesophase towards a microemulsion phase that shows only broad peaks in SAXS.[39] At 8%wt linalool, two bumps still could be distinguished, but long-range structuring was lost. At 10%wt linalool, a single large peak was visible, probably corresponding to a water-poor microemulsion usually labeled as the L2 phase. In the case of flexible surfactant monolayers, this system is labeled Winsor II and is often unstable via emulsification failure

17

that rejects excess water in equilibrium. We are here referring to the case of rigid interfacial films[39] as mentioned previously.
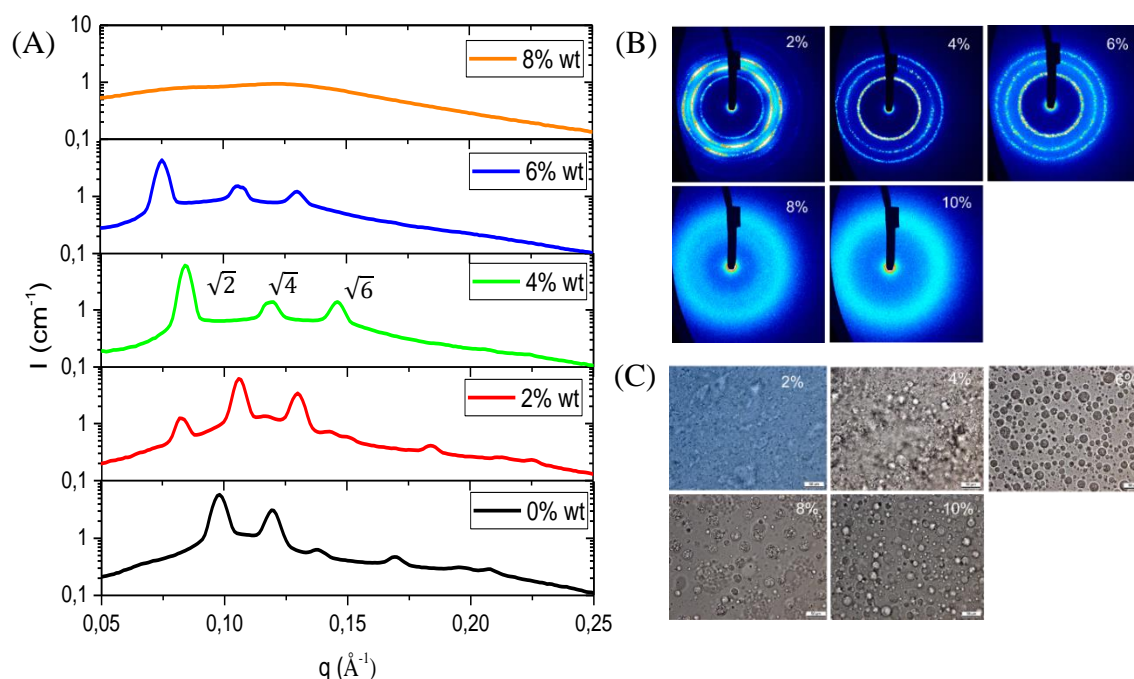

Figure 7 Scattering profiles (A) and 2D patterns (B) of phytantriol-10-GMO-water-linalool mixtures as a function of linalool content. (C) Microscopic images of the bulk gels at 2% and 4%wt linalool and of the spontaneously formed gelified particle dispersions at 6%, 8%, and 10% linalool.

The scattering curve at 2%wt linalool is interesting because the Bragg peak ratios do not correspond to any of the bicontinuous cubic phases. Moreover, the 2D diffraction pattern, presented in Figure 7B, describes a twisted cubic structure such as in the blue cubic phases. This phase should be intermediate between Pn3m and Im3m, having an additional peak at lower q compared with the Pn3m phase. It is surprising that a nonchiral molecule such as linalool induces a twist in the bilayers. However, in previous studies,[40] the transition between P cubic and D cubic phases was studied and it was demonstrated that, during the transition, phase P was rhombohedrally squashed toward the diagonal of the unit primitive cubic cell, which produced the undistorted rhombohedral unit cell of phase D rotated at 60° around the (1;1;1) direction. Therefore, in our case, it seems we exerted the same scenario but inversely, *i.e.* an extension of the D phase on the plane (1;1;1) accompanied by a rotation at 60°, as was demonstrated by Toshihiko Oka.[41] In our case also, we have illustrated that the addition of linalool induced a break in symmetry: the water channels in one direction were preserved and extended, whereas they shrank and disappeared in another direction.

The solubilization of fragrance alcohol into the cubic phase transformed the diamond type to a primitive type of cubic phase with a higher lattice parameter (108 Å at 2% linalool, 106 Å at

4% linalool, and 118 Å at 6% linalool) compared with the lattice parameter without fragrance (91 Å). A higher lattice parameter for the P phase is in accordance with the ratio $a(P)/a(D) = 1,279$ predicted from the condition for conservation of the topology and the total number of unit cells.

The transition from the Pn3m to the Im3m phase could be explained by a change in the Gaussian curvature of the system under the influence of the fragrance molecule. The effective Gaussian curvature ‹ K › of the reversed phases is negative because the effective packing parameter P_{eff} is >1. The relation between the Gaussian curvature and effective packing is given by equation (7).[36] The transition from the Pn3m to the Im3m phase under the action of the fragrance alcohol means a decrease in the Gaussian curvature and therefore, a reduction in P_{eff}.

One possible way to accomplish this is by augmentation of the area per surfactant molecule at the water-lipid interface. This phenomenon has already been observed in different systems: monoolein + sugar esters,[42] and monoolein + oleic acid,[43] where the same transition was induced by the presence of highly hydrophilic polar heads of sucrose ester in the first case and of electrostatic repulsions in the second case. Both examples are characterized by an increased molecular surface area, which decreased the packing parameter. In our situation, the fragrance alcohol is a co-surfactant that adds additional surface area[6–8] to the packing parameter but in the same time it is an oil that adds hydrophobic volume. Thus, it will be solubilized within the hydrophobic part of the bilayer, leading to an increase in the volume of the chains, as well as at the interface, in turn leading to an increase in the surface area. However, the transition to Im3m provides information that the participation of linalool is mainly on the interface, reducing P_{eff} by adding additional surface area per molecule.

Another mechanism that could explain the induced transition is the release of the packing frustration, existing in the Pn3m phase due to the oil solubilization in the hydrophobic domain. As was discussed by Shearman et al.,[44] in the absence of oil, the Pn3m phase should have lower curvature elastic energy than the Im3m phase, but higher chain packing energy. The authors predicted and proved (by the addition of long-chain alkane to the monoolein cubic phase) that the relief of packing stress in the D phase stabilized the P phase. Linalool is an oil and, thus, it can be solubilized in the hydrophobic domain of the Pn3m phase and can induce phase transition by the previously mentioned mechanism as well. Therefore, the surface-active fragrance oil should play the double role of an oil and a co-surfactant. In both scenarios, the actions discussed herein lead to the same result: stabilization of the Im3m phase.

19

The structural parameters of the Im3m phase in the presence of 4%wt linalool are included in Table 4.

Table 4 : Structural parameters for 4% of linalool incorporated in a mixed phytantriol-10-GMO/water Pn3m cubic phase (at 30%wt water composition). The final phase is a Im3m.

Phytantriol+10-GMO in water							
Phase	Linalol %	d* (Å)	a (Å)	l (Å)	lch* (Å)	rw (Å)	$<K>_0$
Im3m	4	74,8	105,8	15,9	8,8	17	-0,0009

With the Euler-Poincare characteristic (Im3m: A_0=2.345 and χ=-4)

The bulk cubic phases disappeared at linalool concentrations above 6%wt. The microscopic images of the samples in Figure 7 containing linalool at concentrations 6, 8, and 10%wt clearly show a dispersion of the cubic phase into gel-like particles. The SAXS analysis of the gel-like phase, extracted after centrifugation of the sample with 6%wt linalool, revealed the presence of an Im3m cubic phase. This proves that the fragrance oil is capable of spontaneously dispersing the cubic phase in smaller particles without destroying the cubic structure and without the need for high-energy treatment. In this way, linalool plays the role of ethanol, already used for spontaneous emulsification of cubosomes.

2.2 Rheological studies

Flow viscosity measurements of the samples containing linalool were performed at low shear rates (below 1 s^{-1}). The aim of these experiments was to evaluate the softness of the gels as a function of linalool concentration. The results are presented in terms of viscosity (Figure 8A) and shear stress (Figure 8B). As can be observed, two groups of viscosity values and behavior could be distinguished: 1) non-Newtonian, pseudoplastic behavior with high viscosity values
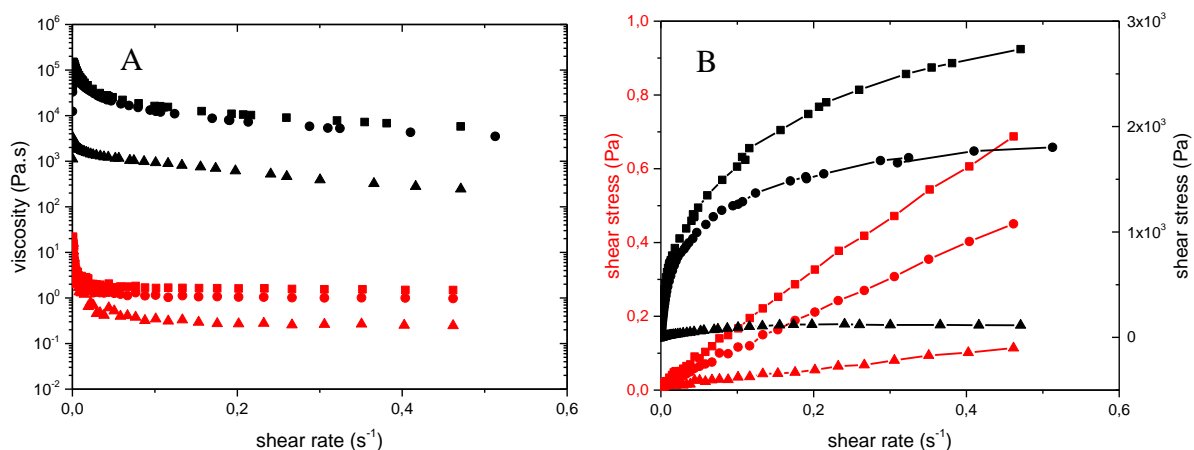
Figure 8 Viscosity (A) and shear stress (B) as a function of low shear rate of the samples containing linalool at concentrations of 0%wt (black squares), 2%wt (black circles), 4%wt (black triangles), 6%wt (red squares), 8%wt (red circles), and 10%wt (red triangles).

at an order of magnitude of 10^3 to 10^5 Pa at 2 and 4%wt, and 2) Newtonian behavior and low viscosity values at an order of magnitude of 1 to 10 Pa at concentrations of 6 to 10%wt linalool. The drastic change in the behavior and viscosity appeared at 6%wt linalool and can be explained by the dispersion of the bulk cubic gel into gelified particles with an excess emulsion phase.

The high softness of the Im3m cubic gel at 4%wt is remarkable. The viscosity is 100 times less than that of the Pn3m cubic gel at 0%wt linalool and the gel is still bulky.

The samples containing 2, 4, and 6%wt linalool showed viscoelastic behavior. The storage and loss modulus curves for 0, 2 and 4%wt linalool are compared in Figure 9. The viscoelastic curves for the sample at 6%wt linalool are included in SI (Figure SI.2.2). Keeping in mind that at 6%wt linalool, the bulk cubic phase was spontaneously dispersed into cubic gel particles, only the viscoelasticity of the extracted by centrifugation cubic gel is presented in Figure SI.2.2.

The values of both G` and G`` moduli are reduced, which corresponds to a softening of the cubic phases with increasing fragrance oil concentration. The relaxation time τ_{max} also decreased progressively from 7.4 s at 0%wt linalool to 1.9 s at 2%wt linalool and 0.26 s at 4%wt linalool.

Viscoelasticity was lost in the samples containing linalool at concentrations higher than 6%wt, which correlates to the SAXS results that indicate the disappearance of the cubic gel.

The temperature dependence of the viscoelastic modulus in the presence of fragrance oil is presented in Figure 9B. As can be observed, the fragrance oil reduces the phase transition T, which appeared at 82°C for the Pn3m mixed cubic phase at 0%wt linalool, significantly to 67°C by adding 2%wt linalool and to 49°C in the presence of 4%wt linalool. A second transition, probably toward an L2 phase, appeared at 56°C on the curves corresponding to the Im3m cubic gel, solubilizing 4%wt linalool. Thus, the transition from Pn3m to Im3m cubic symmetry, induced by the solubilization of 4%wt linalool, created a softer cubic phase but with a reduced T stability range. The cubic gel at 2%wt linalool seems to be an attractive compromise for a well-structured, softer gel with a large T stability range.

Therefore, a fragranced ingredient, especially with an alcohol function, could be used to control the transition T and the softness of the cubic phases.
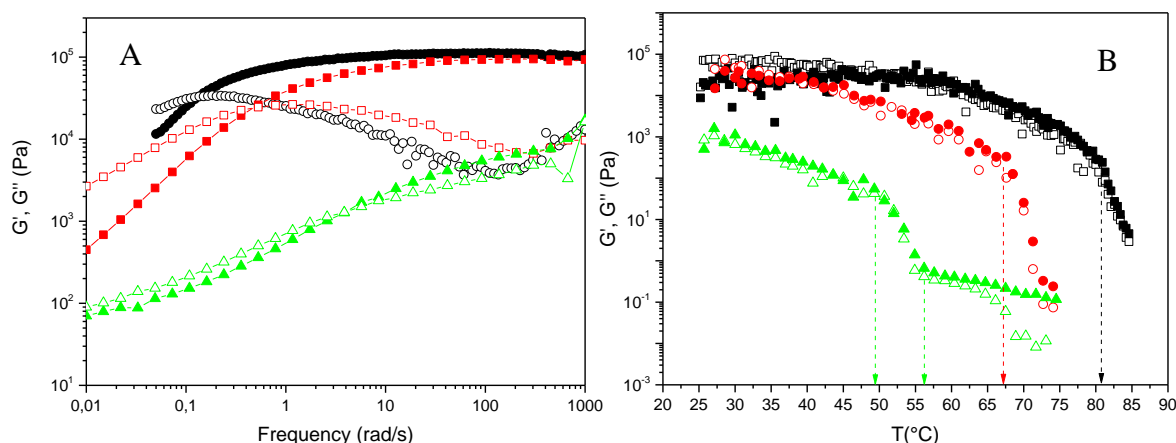

Figure 9 Storage (G`) and loss (G``) modulus of the bulk cubic phases at 0%wt (black), 2%wt (red), and 4%wt (green) linalool as a function of frequency (A) and temperature (B). The dashed arrows in (B) show transition T.

Conclusions

We have presented a way to soften a bulk reversed, cubic, bicontinous gel from a Pn3m type, maintaining its topological structure through a combination of a cubic phase-forming amphiphile (phytantriol) and a lamellar phase-forming (decaglycerol monooleate) amphiphiles. The combination of phytantriol and 10-GMO led to the formation of a Pn3m cubic phase in an extended water concentration range, compared with the cubic phase of the binary phytantriol-water system. The mixed phase has an increased lattice parameter and water channel radius, allowing the solubilization of a higher water quantity. The rheology studies revealed the formation of a softer Pn3m phase with improved temperature stability over a large temperature

range (up to 80°C). The phase transitions from the Pn3m to the hexagonal and L2 phase, observed in the phytantriol-water phase diagram, were displaced above 82°C.

Further, the mixed cubic phase was used for the solubilization of the fragrance oil linalool. We have established that this fragrance molecule, having a surface activity, could induce a Pn3m to Im3m transition via a decrease in Gaussian curvature. Consequently, the viscosity and hardness of the cubic phase are significantly reduced, improving the practical utility of the cubic phase. However, the temperature stability of the cubic phase in the presence of fragrance oil was reduced. An optimum concentration of linalool (2%) was found, at which we obtained a bulk cubic phase with significant viscoelasticity, lower hardness, and good temperature stability (up to 67°C). The cubic phase structure at this concentration of linalool is a twisted "blue" phase structure that appeared as an intermediate phase between the Pn3m and Im3m phases.

A final achievement of this study is the discovery that a surface-active fragrance molecule could spontaneously disperse the bulk cubic phase in the form of cubic particles (cubosomes) acting as a "co-surfactant" similar to that of ethanol.[45] This interesting result could be useful for the insertion of cubic delivery systems in a consumer product such as for personal care.
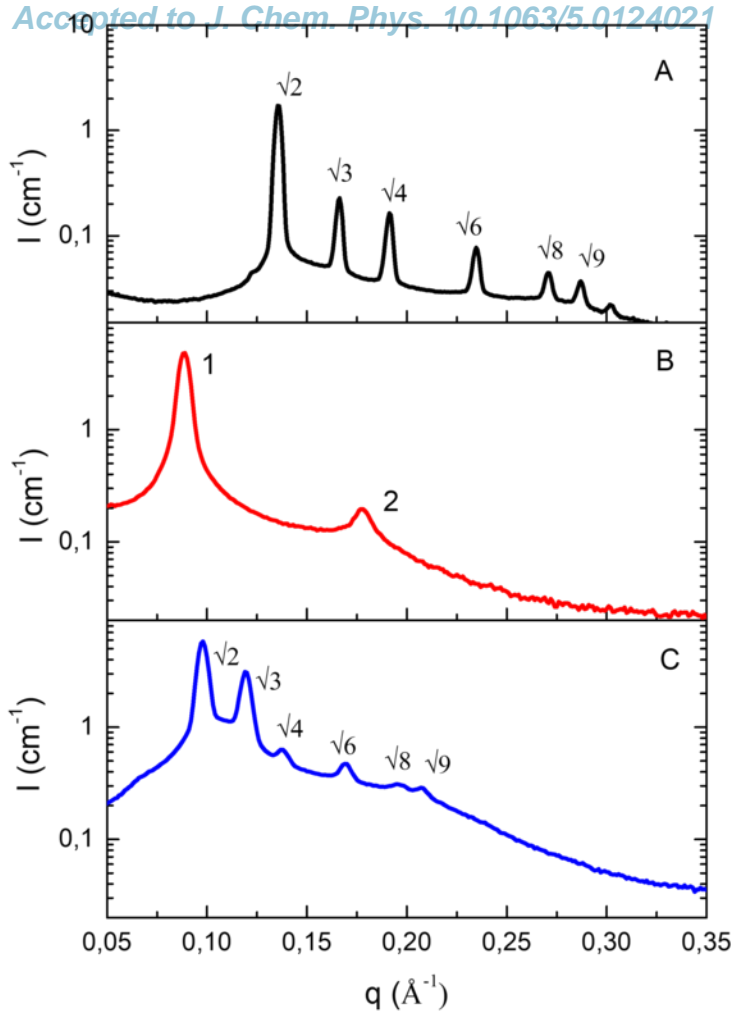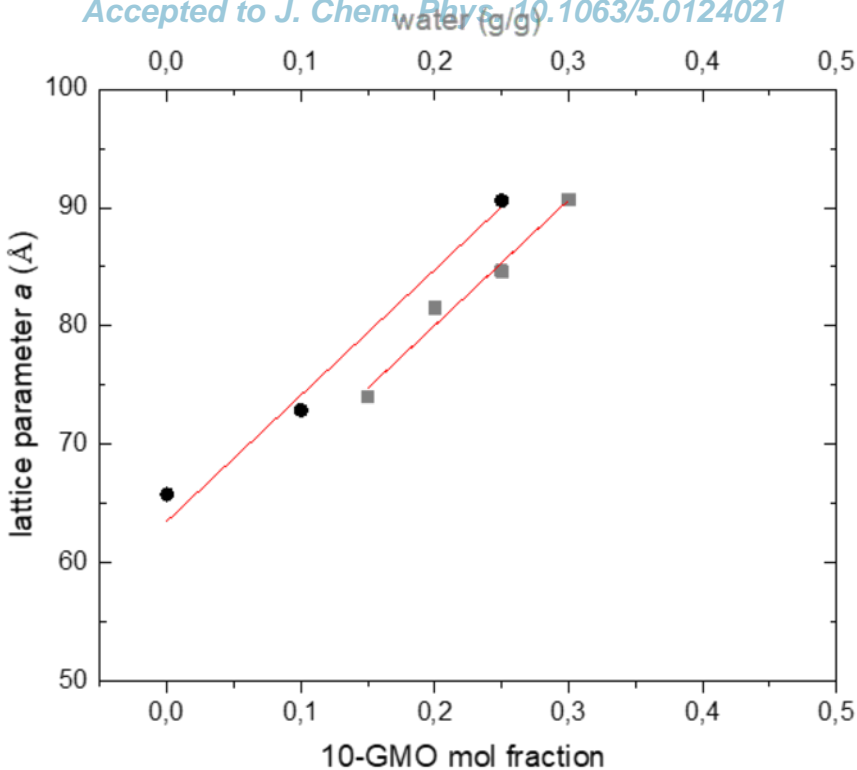
Supplementary Information

The supplementary material contains the equations used for the calculation of the lattice parameters, additional SAXS profiles of the binary systems phytantriol-water and 10-GMO-water, the dependence of the repeat distance as function of the inverse of volume fraction of lipid in lamellar phase of 10-GMO, the SAXS profile of the ternary mixture phytantriol-10-GMO-water at the molar ratio 9:1 of the mixture phytantriol:water, the chemical molecular structure of linalool and the viscoelasticity curve of the sample containing 6%wt linalool.
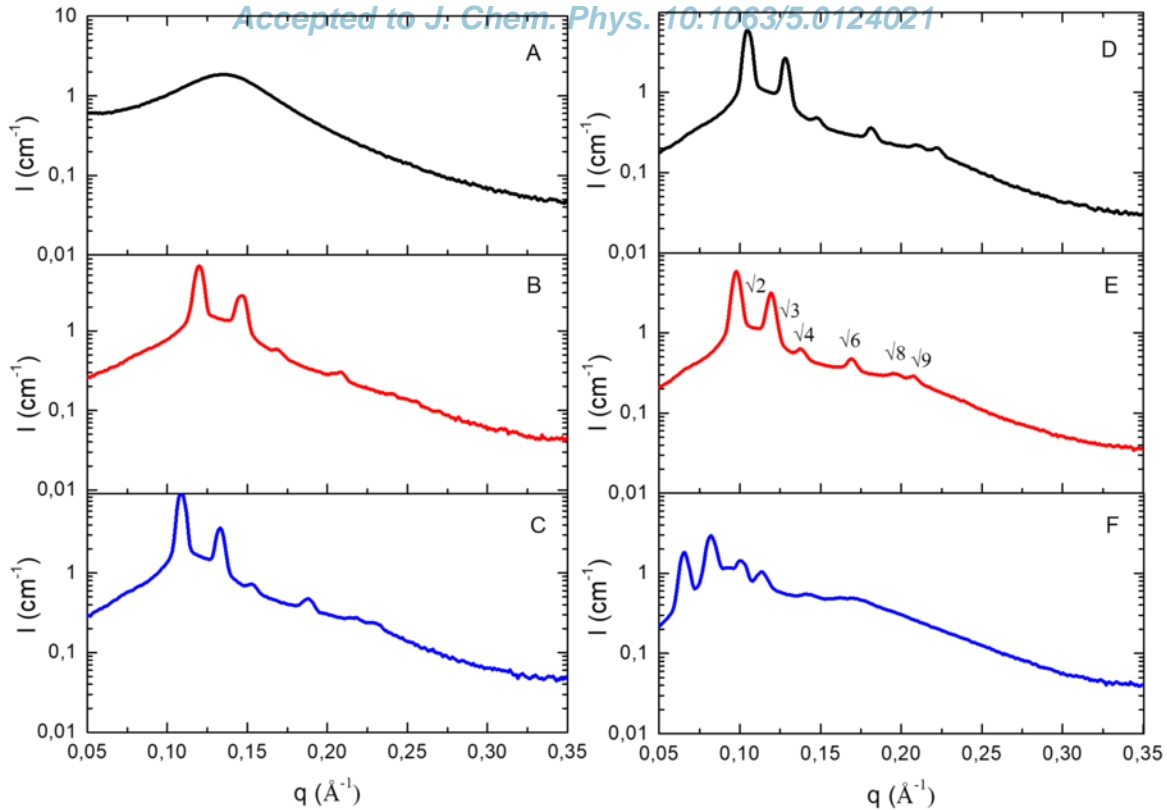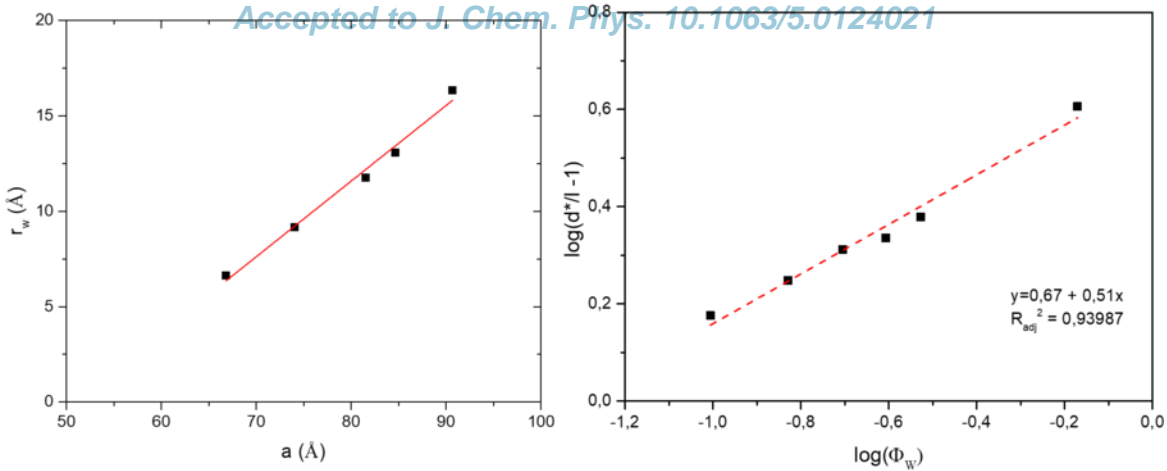
References

[1] R. Mezzenga, J.M. Seddon, C.J. Drummond, B.J. Boyd, G.E. Schröder-Turk, and L. Sagalowicz, Advanced Materials **31**, 1900818 (2019).

[2] B.J. Boyd, in *Bicontinuous Liquid Crystals*, edited by M.L. Lynch and P. Spicer (CRC Press, Boca Raton, 2005), p. 289.

[3] C. Fong, T. Le, and C.J. Drummond, Chem. Soc. Rev. **41**, 1297 (2012).

[4] S. Milak and A. Zimmer, Int. J. Pharm. **478**, 569 (2015).

[5] G. Garg, S. Saraf, and S. Saraf, Biol. Pharm. Bull. **30**, 350 (2007).

[6] V. Tchakalova, F. Testard, K. Wong, A. Parker, D. Benczédi, and T. Zemb, Colloids and Surfaces A: Physicochemical and Engineering Aspects **331**, 31 (2008).

[7] V. Tchakalova, F. Testard, K. Wong, A. Parker, D. Benczédi, and T. Zemb, Colloids and Surfaces A: Physicochemical and Engineering Aspects **331**, 40 (2008).

[8] V. Tchakalova and W. Fieber, J. Surfactants Deterg. **15**, 167 (2012).

[9] V. Rataj, J. Am. Oil Chem. Soc. **98**, 210 (2021).

[10] T. Lukowicz, R.C. Maldonado, V. Molinier, J.-M. Aubry, and V. Nardello-Rataj, Colloid Surf. A-Physicochem. Eng. Asp. **458**, 85 (2014).

[11] N. Kanei, K. Watanabe, and H. Kunieda, J. Oleo Sci. **52**, 607 (2003).

[12] Md.H. Uddin, N. Kanei, and H. Kunieda, Langmuir **16**, 6891 (2000).

[13] M. Kumbhakar, T. Goel, T. Mukherjee, and H. Pal, J. Phys. Chem. B **109**, 14168 (2005).

[14] A. Tidu, F. Meducin, A.-M. Faugere, and S. Guillot, Langmuir **34**, 13283 (2018).

[15] N. Amar-Zrihen, A. Aserin, and N. Garti, J. Agric. Food Chem. **59**, 5554 (2011).

[16] A. Yaghmur, L. de Campo, L. Sagalowicz, M.E. Leser, and O. Glatter, Langmuir **21**, 569 (2005).

[17] J. Borné, T. Nylander, and A. Khan, Langmuir **16**, 10044 (2000).

[18] J. Borné, T. Nylander, and A. Khan, Langmuir **17**, 7742 (2001).

[19] P.J. Maddaford and C. Toprakcioglu, Langmuir **9**, 2868 (1993).

[20] A. Zabara, J.T.Y. Chong, I. Martiel, L. Stark, B.A. Cromer, C. Speziale, C.J. Drummond, and R. Mezzenga, Nat Commun **9**, 544 (2018).

[21] C.V. Kulkarni, W. Wachter, G. Iglesias-Salto, S. Engelskirchen, and S. Ahualli, Phys. Chem. Chem. Phys. **13**, 3004 (2011).

[22] S. Richert, A. Schrader, and K. Schrader, Int J Cosmet Sci **25**, 5 (2003).

[23] T. Zemb, O. Tache, F. Né, O. Spalla, and IUCr, Journal of Applied Crystallography **36**, (2003).

[24] T. Zemb, O. Taché, F. Né, and O. Spalla, Review of Scientific Instruments **74**, 2456 (2003).

[25] J. Barauskas and T. Landh, Langmuir **19**, 9562 (2003).

[26] J.F. Dufrêche and Th. Zemb, Current Opinion in Colloid & Interface Science **49**, 133 (2020).

[27] Hyde S T, in *Handbook of Applied Surface and Colloid Chemistry* (n.d.).

[28] M. Kanduč, A. Schlaich, A.H. de Vries, J. Jouhet, E. Maréchal, B. Demé, R.R. Netz, and E. Schneck, Nat Commun **8**, 14899 (2017).

[29] R. Guo, J. Yang, S.E. Friberg, V. Landeryou, and L. Hall, Journal of Dispersion Science and Technology (2007).

[30] J. Briggs, H. Chung, and M. Caffrey, J. Phys. II France **6**, 723 (1996).

[31] T. Zemb, S. Hyde, P. Derian, I. Barnes, and B. Ninham, J. Phys. Chem. **91**, 3814 (1987).

[32] D.C. Turner, Z.-G. Wang, S.M. Gruner, D.A. Mannock, and R.N. McElhaney, Journal de Physique II **2**, 2039 (1992).

[33] A. Gulik, V. Luzzati, M. De Rosa, and A. Gambacorta, Journal of Molecular Biology **182**, 131 (1985).

[34] C. Speziale, R. Ghanbari, and R. Mezzenga, Langmuir **34**, 5052 (2018).

[35] H. Chung and M. Caffrey, Biophysical Journal **66**, 377 (1994).

[36] S.T. Hyde, J. Phys. Chem. **93**, 1458 (1989).

[37] R. Mezzenga, C. Meyer, C. Servais, A.I. Romoscanu, L. Sagalowicz, and R.C. Hayward, Langmuir **21**, 3322 (2005).

[38] Y. Yao, S. Catalini, B. Kutus, J. Hunger, P. Foggi, and R. Mezzenga, Angew Chem Int Ed **60**, 25274 (2021).

[39] M. Gradzielski, M. Duvail, P.M. de Molina, M. Simon, Y. Talmon, and T. Zemb, Chem. Rev. **121**, 5671 (2021).

[40] A.M. Squires, R.H. Templer, J.M. Seddon, J. Woenkhaus, R. Winter, T. Narayanan, and S. Finet, Phys. Rev. E **72**, 011502 (2005).

[41] T. Oka, Langmuir **31**, 3180 (2015).

[42] R. Negrini and R. Mezzenga, Langmuir **28**, 16455 (2012).

[43] Y. Aota-Nakano, S.J. Li, and M. Yamazaki, Biochimica et Biophysica Acta (BBA) - Biomembranes **1461**, 96 (1999).

[44] G.C. Shearman, B.J. Khoo, M.-L. Motherwell, K.A. Brakke, O. Ces, C.E. Conn, J.M. Seddon, and R.H. Templer, Langmuir **23**, 7276 (2007).

[45] M.L. Lynch and P.T. Spicer, editors , *Bicontinuous Liquid Crystals* (CRC Press, Boca Raton, 2005).